



Published in final edited form as:

J Orthop Res. 2017 December ; 35(12): 2658–2666. doi:10.1002/jor.23587.

Calreticulin inhibits inflammation induced osteoclastogenesis and bone resorption

Charla R. Fischer², Maya Mikami², Hiroshi Minematsu², Saqib Nizami², Heon Goo Lee², Danielle Stamer¹, Neel Patel¹, Do Yu Soung², Jung-ho Back¹, Lee Song², Hicham Drissi³, Francis Y. Lee¹

¹Department of Orthopaedic Surgery and Rehabilitation, Center for Musculoskeletal Care, Yale University School of Medicine, 47 College Street, New Haven, New York

²Robert Carroll and Jane Chace Carroll Laboratories, College of Surgeons and Physicians of Columbia University, 650 W. 168th Street, BB14-1412, New York, NY 10032

³Department of Orthopedic Surgery, Emory School of Medicine, Atlanta, GA

Abstract

Osteoclasts play key roles in bone remodeling and pathologic osteolytic disorders such as inflammation, infection, bone implant loosening, rheumatoid arthritis, metastatic bone cancers, and pathological fractures. Osteoclasts are formed by the fusion of monocytes in response to receptor activators of NF- κ B-ligand (RANKL) and macrophage colony stimulating factor 1 (M-CSF). Calreticulin (CRT), a commonly known intracellular protein as a calcium-binding chaperone, has an unexpectedly robust anti-osteoclastogenic effect when its recombinant form is applied to osteoclast precursors *in vitro* or at the site of bone inflammation externally *in vivo*. Externally applied Calreticulin was internalized inside the cells. It inhibited key pro-osteoclastogenic transcription factors such as c-Fos and nuclear factor of activated T cells, cytoplasmic 1 (NFATc1) in osteoclast precursor cells that were treated with RANKL *in vitro*. Recombinant human Calreticulin (rhCRT) inhibited lipopolysaccharide (LPS)-induced inflammatory osteoclastogenesis in the mouse calvarial bone *in vivo*. Cathepsin K molecular imaging verified decreased Cathepsin K activity when rhCalreticulin was applied at the site of LPS application *in vivo*. Recombinant forms of intracellular proteins or their derivatives may act as novel extracellular therapeutic agents. We anticipate our findings to be a starting point in

Author Contributions:

Charla Fischer: Data Analysis and manuscript writing

Maya Mikami: Proteomic analysis, electrophoresis

Hiroshi Minematsu: Proteomic analysis, cell culture

Saqib Nizami: Cathepsin K imaging, cell culture, *in vivo* experiments, histology, writing and editing

Heon Goo Lee: *in vivo* experiments, histology

Danielle Stamer: Data Analysis and Manuscript Writing

Neel Patel: *in vivo* experiments

Do Yu Soung: PCR, editing

Jung-ho Back: Cell Culture

Lee Song: Immunofluorescence microscopy, cell culture, PCR and protein experiments, writing and editing

Hicham Drissi: Study direction, writing and editing

Francis Y. Lee: Data Analysis, Interpretation, Manuscript Preparation, Revision, and Supervision as PI

This paper was the recipient of the 2016 Kappa Delta Ann Doner Vaughn Award

unraveling hidden extracellular functions of other intracellular proteins in different cell types of many organs for new therapeutic opportunities.

Keywords

Osteoclasts; Calreticulin; bone; inflammation

Introduction

Osteoclasts are bone resorbing cells formed by the fusion of monocytes in response to cytokines, such as RANKL and MCSF, produced by osteoblasts, osteocytes, T cells, synovial cells, cancer cells, or periodontal cells¹. Osteoclast production is a normal component of the bone resorption and bone deposition balance that keeps skeletal health in check. However, wayward osteoclastogenesis tilts the balance towards excess bone resorption and is thereby responsible for many medical and dental pathologies such as osteomyelitis, implant loosening, periodontitis, metastatic bone cancers, and inflammatory arthritis²⁻⁴. Osteoclastogenic formation and function has intrigued many clinicians and scientists, partly due to the multifarious cell types implicated in osteoclast formation, which afford many avenues of inquiry.

Therapeutics dealing with reigning in resorptive functions have been an evolving research concept for the past 30 years⁵⁻⁷. Bisphosphonates either in the form of oral pills or intravenous drugs have been widely used for the treatment of osteoporosis and metastatic bone cancers. This has led to increased awareness of bisphosphonate-related side effects such as atypical subtrochanteric fractures, avascular necrosis of jaw bone, and renal toxicity⁸. Osteoprotegerin (OPG) is a decoy receptor for RANKL and was being pursued as an anti-osteoclastogenic therapeutic agent, but it eventually lost favor as clinical trials demonstrated the production of antibodies in response to exogenous OPG^{9; 10}. As knowledge of bone biology increased, potential therapeutics along newly defined pathways were sought. Denosumab, a recombinant RANK:Fc that competitively inhibits RANKL-RANK binding, emerged as a new therapeutic that blocks osteoclast formation. However, denosumab is associated with atypical fractures, avascular necrosis of jaw bone, immunologic side effects such as dermatitis, and other complications¹¹⁻¹³. Another promising avenue of research comes from compounds normally outside of osteoclastogenic pathways. Parathyroid Hormone (PTH) exhibited paradoxical bone anabolic effects with daily injection in rats in 1929¹⁴. This was surprising as the established wisdom indicated that overexposure to PTH would effect a net bone loss. The paradox was subsequently largely ignored and research lay dormant until the FDA approved daily subcutaneous injection of PTH (“intermittent PTH”) for the treatment of osteoporosis. However, while it can be an effective therapy, the anabolic activity has a potential side effect of enhancing cancer growth¹⁵. There is a near-constant need to develop new, more effective, safer therapeutics to protect bone in bone-resorbing disorders. The history of bone therapeutics has demonstrated that sometimes the search for new treatments requires uncommon uses of common endogenous compounds.

In pursuit of new therapeutics, we identified Calreticulin (CRT) as a potential anti-resorptive protein through proteomic screening of osteoclast precursors treated with RANKL. CRT is known as a calcium binding intracellular protein and has been implicated in muscle diseases and phagocytosis of cancer cells by macrophages¹⁶. CRT is also a highly conserved protein that is preserved in plants and mammalian cells¹⁷. Overexpression of CRT in plants exhibits resistance to cold weather or drought¹⁸. Most existing literature defines CRT as a classical endoplasmic reticulum resident protein that regulates cytoplasmic and endoplasmic reticulum calcium levels. Furthermore, many diverse roles have been described for CRT as an intracellular protein in cardiac development cell proliferation, matrix synthesis, adaptive immune response, atherosclerosis, and cancers^{19–21}. There is far less data on an extracellular non-classical function of CRT. One study showed that exogenous CRT accelerated wound healing in pigs when it was applied at the site of skin injury²².

In this study, we examined whether exogenous Calreticulin is a potent inhibitor of osteoclastogenesis by blocking key pathways osteoclastogenesis *in vitro*. We further investigated if regional administration of CRT results in inhibition of LPS-induced osteoclast function *in vivo*.

Materials and Methods

Reagents

Mouse macrophage cell line RAW264.7 from American Type Culture Collection (ATCC, Manassa, VA) cultured in complete DMEM. Recombinant human Calreticulin (rhCRT) with His tag purchased from Abcam (Cambridge, MA). Caspase-1 inhibitor Ac-YVAD-CMK was purchased from Enzo Life Sciences (Farmingdale, NY). Cell culture media, such as Dulbecco's Modified Eagle Medium (DMEM) and Minimum Essential Media alpha (MEM α), PBS, and Penicillin-Streptomycin (10,000U/ml) were from Gibco, Life Technologies (Grand Island, NY). Heat inactivated fetal calf serum (FCS) was from HyClone Technologies (Fisher Scientific, Pittsburg, PA). DMEM or MEM α was supplemented with 10% FCS and 100ug/ml penicillin plus 100U/ml streptomycin (Gibco). Cytokine M-CSF and RANKL are from Shenandoah Biotechnology Inc. (Warwick, PA). Lipopolysaccharide (LPS from *E. coli* K12) was from InVivoGene (San Diego, CA). Endotoxin removal kit was from Norgen Biotek (Thorold, Ontario, Canada). HyStem-C hydrogel was from ESI BIO (Alameda, CA). RNA was extracted using RNeasy mini kit (QIAGEN, Valencia, CA), and cDNA reverse transcribed into cDNA using Maxima First Strand cDNA synthesis kit (Thermo Scientific), and quantified using Light Cycler Fast Start DNA Master Plus SYBR Green 1 (Roche, Indianapolis, IN) with Realplex Mastercycler eppgradient S PCR machine (Eppendorf, Hauppauge, NY). RIPA buffer, Thermo Scientific™ Halt™ Combined Protease and Phosphatase Inhibitor Cocktails, and Super Signal West Femto Maximum Sensitivity Substrate were from Thermo Scientific (Rockford, IL). Antibodies against mouse NFATc1, c-Fos, phosphor-CREB (cAMP responsive element binding protein) and total CREB, GAPDH for western blot were purchased from Cell Signaling Technology (Danvers, MA). Anti-6x His and anti-Calreticulin antibodies are from Abcam, and Alexa Fluor-488 conjugated secondary antibody for immunofluorescence microscopy is from Life Technologies (Grand Island, NY). TRAP staining was carried out

with Leukocyte Acid phosphatase (TRAP) kit from Sigma-Aldrich (St. Louis, MO). RhCRT released from hydrogel was measured by ELISA (LifeSpan Biosciences, Inc., Seattle, WA). Wild type C57B16/J, and NOD mice, aged from 6 to 10 weeks, were purchased from Jackson Laboratory (Bar Harbor, ME). All the experiments involved with mice had been approved by the Institutional Animal Care and Use Committee (Protocol AC-AAAD2253).

Cell culture

Bone marrow derived osteoclasts (BMOCs) were made as previously reported²³. Bone marrow cells from six to nine weeks old C57B16/J and NOD male mice were flushed from the femur with media and seeded overnight in complete MEM α . The floating progenitor cells were cultured in complete MEM α media complemented with M-CSF (10~30ng/ml) for two days. The cells were then differentiated into osteoclasts by treating with M-CSF (10~30ng/ml) and RANKL (50ng/ml, Shenandoah Biotechnologies) for three days with one media change after two days. The inhibitors were added at the time of RANKL treatment. Mature osteoclasts were then stained with a TRAP staining kit (Sigma Aldrich) according to manufacturer's instruction. TRAP positive cells with greater than three nuclei were counted as mature osteoclasts. RNA was extracted with RNAeasy kit (Qiagen), and whole cell lysates were made with RIPA buffer (Thermo Scientific) or stained with different antibodies using immunofluorescence (see below).

Proteomic analysis

Mouse bone-marrow derived monocytes were grown in M-CSF (10ng/ml) for two days, then the cells were treated either with M-CSF, caspase-1 inhibitor YVAD, RANKL (50ng/ml), or YVAD and RANKL combined for 24 hours. Total cell lysate was harvested with RIPA buffer and subjected to a 2 dimensional gel electrophoresis with a pH gradient that ranged from 3.5 to 10, and 10% SDS-PAGE. The gels were then stained with Coomassie Brilliant Blue (Biorad) and the differentially expressed protein bands were cut, digested with trypsin, and subjected to liquid chromatography combined with mass spectrometry (LC-MS/MS) at the CUMC Proteomics Center. The proteins were identified using Matrix Science's Macot database search tool (http://www.matrixscience.com/search_form_select.html).

Immunofluorescence microscopy

Bone-marrow derived cells were grown in a four-chamber polystyrene vessel tissue culture treated glass slide (BD Falcon, Bedford, MA) for 2 days in complete MEM α supplemented with M-CSF (10ng/ml) and then for one day with M-CSF (10ng/ml) plus RANKL (100ng/ml) with or without rhCRT-His (4 μ g/ml). The cells were then briefly washed with cold PBS and fixed in 4% formaldehyde. To detect surface (extracellular) CRT, the cells were stained with rabbit anti-6x His or anti-Calreticulin antibody (1:50); to detect intracellular and extracellular Calreticulin, the cells were stained with the same antibodies as above after the cells were permeabilized with 0.05% Tween 20 in PBS. The target His tag or Calreticulin was detected by anti-rabbit Alexa Fluor 488 antibody. The confocal images were taken using a Zeiss LSM 510 META Confocal Microscope.

In vivo calvarial bone inflammation and resorption

The *in vivo* calvarial osteolysis model has been reported on previously²⁴. We modified existing animal models by using a hydrogel (HyStem-C, EsiBio, CA) for sustained inflammation-associated bone loss and as a concurrent drug delivery system. An advantage of hydrogel is site-specific distribution of LPS or therapeutic agents in the area where the gel lies over the calvarial bones (Figure 1a). Scanning Electron Microscopy of the hydrogel illustrated a pocked gel surface (Figure 1 b) after seven days, which allowed for the sustained low-level release of therapeutic agents, such as human recombinant CRT. The release of rhCRT from the hydrogel was measured with ELISA over a four-day period, and illustrates a sustained release over that timespan (Figure 1 b, graph). Nine-week-old wild type C57Bl/6J mice (N=5) were injected with LPS (2mg/kg) with or without rhCRT (0.2mg/kg) in hydrogel into pericranium of calvaria; the control group was injected with hydrogel only (Figure 1b and 1c). We verified the retention of methylene blue-loaded hydrogels in the region of interest over the calvarial bone *in vivo*. Gross dissection specimens demonstrated the retention of gels at the injection sites to minimize non-specific diffusion of materials. When LPS was delivered, sustained inflammatory responses characterized by aggregates of cells and osteoclastic bone resorption were consistently observed (Figure 1d). The use of hydrogels did not affect the Cathepsin K molecular imaging or the therapeutic effects of therapeutic agents of interest. Then, the calvaria was removed and fixed in 3.7% paraformaldehyde overnight, and de-calcified in 10% EDTA for seven days. The decalcified calvaria was then sectioned and stained with TRAP (Sigma-Aldrich) or Haematoxylin and Eosin. The kinetics of CRT released from hydrogel were carried out in PBS. After seven days at 37°C, crater-like holes were found on the surface of hydrogel. Recombinant human CRT released from hydrogel was measured by ELISA.

Ca²⁺ oscillation

Intracellular Ca²⁺ oscillation was measured as previously reported with small modifications^{23, 39–41}. Mouse bone-marrow derived cells were seeded in a 10cm cell culture plate overnight. The next day, the floating cells were plated onto a 35mm glass bottom culture dish (MatTek corp, Ashland, MA) with M-CSF (10ng/ml) for two days, and the medium was then changed to a medium containing M-CSF (20ng/ml) and RANKL (80ng/ml) with or without CRT for three more days with one medium change after 48 hours. On the last day, the cells were labeled with 5uM Fluo4-AM, 5uM FuraRed, 0.02% Pluronic F127 in phenol red free, serum free MEM α in 37°C for 30 minutes. The cells were then washed 2 times with complete MEM α , and stimulated with RANKL (80ng/ml) in complete MEM α for 20 minutes. The cells were then washed 3 times with Hank's buffer saline solution (HBSS), and 2 ml of recording medium (NaCl 115 mM, KCl 5.4 mM, MgCl₂ 1 mM, CaCl₂ 2 mM, Glucose 10 mM, and HEPES 20 mM, pH 7.4) was added. Ca²⁺ oscillation was observed and recorded every 2 seconds over 10 minutes using Nikon's N-Storm Spinning-Disk TIRF microscope, and Ca²⁺ was reported as the ratio of fluorescent intensities between Fluo4 AM and FuraRed after background subtraction. To see if CRT could inhibit Ca²⁺ transport across the cell membrane, 5 uM of ionomycin was added to the cells at 7 minutes 15 seconds.

Cathepsin K imaging *in vitro* and *in vivo*

RAW264.7 cells were cultured in a 96-well plate for three days. The cells were either left untreated, treated with RANKL, Calreticulin, or RANKL combined with Calreticulin in triplicates. After three days, the Cathepsin K 680 Fast Fluorescent Imaging Agent (Perkin Elmer Life and Analytical Sciences, Shelton, CT) was added at 2M and quantified after 30 minutes using Kodak In-Vivo Multispectral Imaging System (Bruker, CT). The Cathepsin K activity was presented as the intensity of the signal in the region of interest (ROI).

In vivo Cathepsin K Imaging was conducted for the calvarial osteolysis models in order to monitor osteoclast activity. Animals were given a 2M dose of Cathepsin K 680 Fast Fluorescent Imaging Agent through a tail vein injection. This probe was allowed to circulate for 6 hours, and hair was removed from the skin on the calvarial region to reduce signal noise. The In-Vivo FX Imaging System (Bruker, CT) was used to take X-rays and Fluorescent Near-Infrared images of the mouse; an ROI was established corresponding to the area where the hydrogel had been loaded. The optical signal was then quantified and normalized against the background signal of each mouse.

Statistics

All the data are presented as mean±standard error in bar graphs. The statistical significance between the treatments was determined by one-way ANOVA and student T-test. Post-hoc analysis, after the one-way ANOVA, was carried out by implementing Dunnett's test on treatment groups against control, to determine significant confidence intervals for treatments. The mean of each experimental group was compared to the mean of the control group and a confidence interval for each comparison is generated through Dunnett's method which illustrates significance.

Results

Proteomic identification of Calreticulin, which was associated with inhibition of osteoclastogenesis by Ac-YVAD-CMK

Our initial investigations showed that the caspase 1 inhibitor, Ac-YVAD-CMK, blocked RANKL-induced osteoclastogenesis in a dose-dependent manner *in vitro* and *in vivo* (data not shown). This finding advanced our goal of identifying new anti-osteoclastogenic compounds. A two-dimensional gel electrophoresis of proteins from osteoclast precursors treated with RANKL, Ac-YVAD-CMK, or RANKL + Ac-YVAD-CMK resulted in a significant increase in a particular protein band's density under Ac-YVAD-CMK treatment conditions (Figure 2 a). After LC-MS/MS analysis of the recovered band, the protein was identified as Calreticulin (CRT).

Further experimentation was required to establish and elucidate CRT's role in osteoclastogenesis. *In vitro* osteoclastogenesis using mouse BMMs treated with M-CSF with or without RANKL clearly demonstrated that the addition of recombinant human CRT-inhibited, RANKL-mediated osteoclast formation in a dose-dependent manner (Figure 2 b and c). To functionally illustrate this inhibition, we utilized the Cathepsin K 680 FAST Fluorescent imaging agent. After three days of treatment with RANKL on

RAW264.7, Cathepsin K activity increased by approximately twofold (Figure 2 e, left panel). Recombinant human CRT administration halted this increased Cathepsin K activity (Figure 2 e, right panel). Quantitative real-time PCR indicated inhibition of TRAP (Tartrate Resistant Acid Phosphatase, Acp5), Cathepsin K (CtsK), and Matrix Metalloprotease 9 (MMP9) gene expression after the addition of CRT to RANKL treated RAW264.7 cells (Figure 2 f).

Exogenous Calreticulin was taken up by osteoclast precursors and inhibited osteoclast formation

In order to mechanistically narrow down this inhibition, we assessed whether exogenous recombinant CRT acts through interacting with the cell surface or by trafficking into the cell. We used His-tagged recombinant human CRT and an anti-His antibody to distinguish exogenous CRT from endogenous CRT. His-tagged CRT was quickly internalized after addition to the mouse macrophage cell line RAW264.7 cells. Within five minutes, His-tagged CRT was seen inside cells (Figure 2 d). In untreated cells, CRT antibody stained endogenous CRT in RAW264.7 cells while these cells remained negative when incubated with the anti-His antibody. Exogenous recombinant His-tagged CRT was present throughout the cytoplasm, suggesting that exogenous CRT was internalized. To establish that CRT administration is not cytotoxic, an MTT assay was carried out (Supplementary Figure 1). The exogenous CRT itself was not toxic in the given dose range. The internalization of exogenous CRT and subsequent inhibition of osteoclastogenesis indicates that CRT-based osteoclastogenic inhibition is not at the cell surface RANKL-RANK blocking but through intracellular interactions.

Increased availability of CRT inhibits osteoclastogenesis

Having established that recombinant CRT can transit inside the cells, we then examined whether viral over-expression of CRT inside the cells could also inhibit osteoclastogenesis. We generated lentiviral vectors that either expressed GFP protein alone (control) or co-expressed with CRT (Figure 2 g). The RAW264.7 cells were then transduced with or without either the GFP empty vector or with the bi-cistronic CRT-GFP vector. Overexpression of CRT transduced RAW264.7 cells was confirmed by western blot (Figure 2 g). Transduced cells were then treated with RANKL for three days and osteoclasts were identified by TRAP staining. RAW264.7 cells over-expressing CRT displayed repressed osteoclast formation in response to RANKL (Figure 2 g). The data indicate that CRT is an inhibitor of osteoclastogenesis induced by RANKL.

Recombinant Calreticulin inhibits osteoclastogenesis by inhibiting NFATc1 and Ca²⁺ oscillation

To determine the mechanisms by which recombinant CRT inhibits osteoclastogenesis, we first checked the transcription factors that are known to mediate osteoclastogenesis. RAW264.7 cells were treated with RANKL for three days without or with recombinant CRT, and total protein lysates were subjected to SDS-PAGE and probed with antibodies against NFATc1, c-Fos, CREB, and I κ B. As expected, RANKL treatment increased the expression of NFATc1 and c-Fos, two key transcription factors for osteoclastogenesis. C-Fos has a critical role in RANKL-mediated induction of NFATc1, which then translocates

to the nucleus and increases levels of NFATc1 and other osteoclast specific genes. This auto-amplification of NFATc1 drives terminal osteoclast differentiation²⁵. CRT almost completely blocked auto-amplification of these two transcription factors in response to RANKL. Other signaling pathways involving CREB and NF- κ B were not affected by CRT treatment in osteoclast precursors that were treated with RANKL (Figure 3 a). Further experimentation was needed to establish a timeline of the CRT mechanism. We treated RAW264.7 cells with RANKL with and without recombinant CRT and assessed NFATc1 expression over 72 hours. NFATc1 protein level was significantly increased 48 hours after RANKL treatment (Figure 3 b, top panel), while CRT completely blocked its synthesis at 48 hours, and the inhibition lasted to 72 hours, suggesting sustained inhibition. NFATc1 auto-amplification is known to depend on intracellular Ca²⁺ oscillation^{26; 27}. To examine whether the inhibition of NFATc1 by CRT interferes with Ca²⁺ signaling, we measured relative Ca²⁺ oscillation in primary mouse BMMs treated with RANKL in the absence or presence of recombinant CRT. Intermittent spikes represent RANKL-induced Ca²⁺ oscillation (Figure 3c, upper graph). The relative vertical amplitudes diminished significantly when CRT was exogenously added (Figure 3 c, lower graph). However, CRT did not inhibit ionomycin-induced Ca²⁺ influx (a downward vertical arrows in Figure 3c), suggesting a selective effect of CRT on intracellular calcium signaling.

Exogenous CRT blocks inflammation-associated osteoclastogenesis in vivo

We utilized a LPS-induced mouse calvaria model to determine whether recombinant CRT can inhibit inflammatory osteolysis *in vivo*. As expected, LPS inoculation induced significant osteoclast formation and bone resorption in the first three days of treatment. This was evidenced by increased number of TRAP⁺ osteoclasts (Figure 4, top). The addition of CRT blocked this LPS-induced bone resorption (Figure 4, top). As a protease involved in the breakdown of bone matrix and collagens, Cathepsin K is a good indicator of functioning osteoclasts^{28; 29}. Fluorescent imaging for Cathepsin K activity was employed to assess functional osteoclast activity. This activity was measured using Cathepsin KTM 680 Fast Fluorescent Imaging Agent that emits quantifiable light that is proportional to Cathepsin K activity. Consistent with TRAP staining results, calvaria from LPS-treated mice had higher Cathepsin K activity, which then diminished with CRT treatment (Figure 4). The data indicate that recombinant CRT can inhibit the inflammatory osteoclastogenic function in this model of LPS-induced osteolysis.

Discussion

CRT is a 417 amino acid, 46-kDa protein with middle P- and C-terminal domains with multiple calcium interacting sites. The N- and C-terminal domains contain sites for endoplasmic reticulum¹⁹. CRT is known to play various roles in human development, physiology, and diseases. It was first identified in the rabbit skeletal muscle sarcoplasmic reticulum through calcium-binding affinity experiments³⁰. CRT functions have been studied as an intracellular protein in plants and mammals, both of which share significant homology. CD91 was suggested as a co-receptor for CRT and heat shock proteins³¹. Although the mechanisms are not clear, exogenous CRT rescues defective functions in adhesion, migration, and cell signaling in CRT-null mice¹⁶. There are only a few studies on the effect

of exogenous CRT on pathology or wound repair. Exogenous CRT is known to increase proliferation and migration of keratinocytes and endothelial cells during wound healing in porcine skin defects²². Another study showed that exogenous CRT protects balloon catheter-induced arterial injury by preventing intimal hyperplasia in rats³². In these studies, the exact signaling mechanism by which exogenous CRT binds to receptors is unclear, but there is nevertheless a pronounced and demonstrable effect. In our study, immediate intracellular localization of CRT suggests that anti-osteoclastogenic function is through intracellular interactions. However, a mechanism responsible for trans-membrane transport and intracellular mobilization is unclear at the present time.

We were able to add to the growing pool of knowledge on exogenous CRT by examining its function in the regulation of osteoclastogenesis in the context of bone inflammation. Our investigation of Calreticulin grew out of experiments designed to screen for molecules interacting with the osteoclastogenic suppressor, Ac-YVAD-CMK. The goal of these experiments was to identify and subsequently vet compounds with untapped anti-osteoclastogenic capabilities. Our 2D gel screening strategy used osteoclast precursors in the presence and absence of RANKL and anti-osteoclastogenic agent Ac-YVAD-CMK. We identified CRT as the most differentially expressed protein in association with inhibition of osteoclastogenesis. Any potential therapeutic must pass through the rigors of *in vitro* and *in vivo* testing; therefore, we developed an *in vivo* proof of concept. We adopted a mouse calvaria model of LPS-induced inflammatory bone loss²³ to examine the anti-osteoclastogenic function of externally applied recombinant Calreticulin at the site of inflammatory osteolysis *in vivo*. We used a hydrogel-based, sustained, and controlled delivery system to retain LPS or Calreticulin at the target location, eliminating the need for repeat injections. This model demonstrated, for the first time, an essential function for CRT as a potent inhibitor of inflammatory osteolysis.

In order to determine whether exogenous CRT was acting extra- or intracellularly, we placed a –His tag on the protein. Confocal microscopy showed that the exogenous CRT was imported into the cell to effectively halt RANKL-induced osteoclastogenesis *in vitro*. These experiments demonstrated the viability of exogenous CRT as an anti-osteoclastogenic agent that can potentially prevent, or at least significantly decrease, the formation and function of pathologic osteoclasts.

As we delved further into the molecular mechanisms of CRT's anti-osteoclastogenic effect, we showed that CRT inhibited c-Fos and auto-amplification of NFATc1, two crucial signaling processes during osteoclastogenesis in response to RANKL³³. We made attempts to identify the anti-osteoclastogenic domain by making different-length CRT fragments based on the linear N-, P-, and C-terminal domains, but to no avail (data not shown). Further experimentation is required to determine whether there is a specific anti-osteoclastogenic sequence in a 3-dimensional structure. Regarding downstream effector molecules of exogenous CRT, we conducted proteomic assays and identified several proteins that co-immuno-precipitated with CRT after RANKL treatments in macrophages. Those proteins are Ras GTPase-activating-like protein (IQGAP1), involved in vascular remodeling, angiogenesis, and macrophage infiltration^{34–36}. IQGAP1 inhibits dephosphorylation of NFATc1, a critical event for osteoclastogenesis^{23; 25; 27}. Dephosphorylation of

NFATc1 prompts nuclear translocation of NFATc1, transcribing target genes such as NFATc1 itself and Cathepsin K. RANKL induces intracellular Ca^{2+} concentration change, turning on phosphatase Calcineurin which then dephosphorylates NFATc1 in cytoplasm. Dephosphorylated NFATc1 then translocates into the nucleus to transactivate its own promoter and subsequently increase its production. Exogenous CRT may bind to IQGAP1, thereby making detachment from NFATc1 difficult. More experimentation would be needed to dissect further signaling pathways.

Cathepsin K is one of the effector enzymes that degrade bone. Molecular imaging of osteoclastic activity is a desired modality to detect sites of pathologic bone resorption such as periprosthetic bone resorption, periodontitis, or osteolytic metastatic bone cancers. We verified a concept of functional osteoclastic imaging by correlating osteoclastogenesis *in vitro* and *in vivo*. Exogenous CRT effectively inhibited LPS-induced inflammatory osteoclastic bone resorption *in vivo*. Therefore, both *in vitro* and *in vivo* models demonstrated inhibited osteoclastogenesis with exogenous CRT administration. This research opens avenues to CRT-based therapeutics that can promote protection from inflammatory events.

Our study also began revealing the unknown extracellular functions of intracellular signaling proteins as potential therapeutics (Figure 5). Although trans-membrane transportation is currently unclear, recombinant Calreticulin enters the cells and interferes with key osteoclastogenic events such as NFATc1 auto-amplification, Ca^{2+} oscillation induced by RANKL, and c-Fos activation. As a first step for therapeutic exploration of naturally present intracellular proteins, we strategically examined direct interactions between locally applied recombinant CRT and inflammatory osteolysis in the murine calvarial region. Systemic administration of CRT-based peptides will be the subject of further investigation.

Collectively, the data in this study highlight a new way of expanding therapeutic opportunities by unraveling extracellular functions of commonly granted intracellular proteins. One such example of different intra- and extracellular functions is seen in progranulin³⁷. Recombinant progranulin, given in the setting of inflammatory arthritis, unexpectedly turns out to be a TNF-signaling modifying agent by inhibiting TNFR1 but enhancing TNF2 signaling³⁸. Even the most commonly regarded intracellular proteins may exhibit distinct biological or therapeutic functions when they are delivered through extracellular compartments, reminiscent of the use of DNAs or siRNAs as therapeutic agents.

Supplementary Material

Refer to Web version on PubMed Central for supplementary material.

Acknowledgments

National Institutes of Health for research support (R01AR056246)

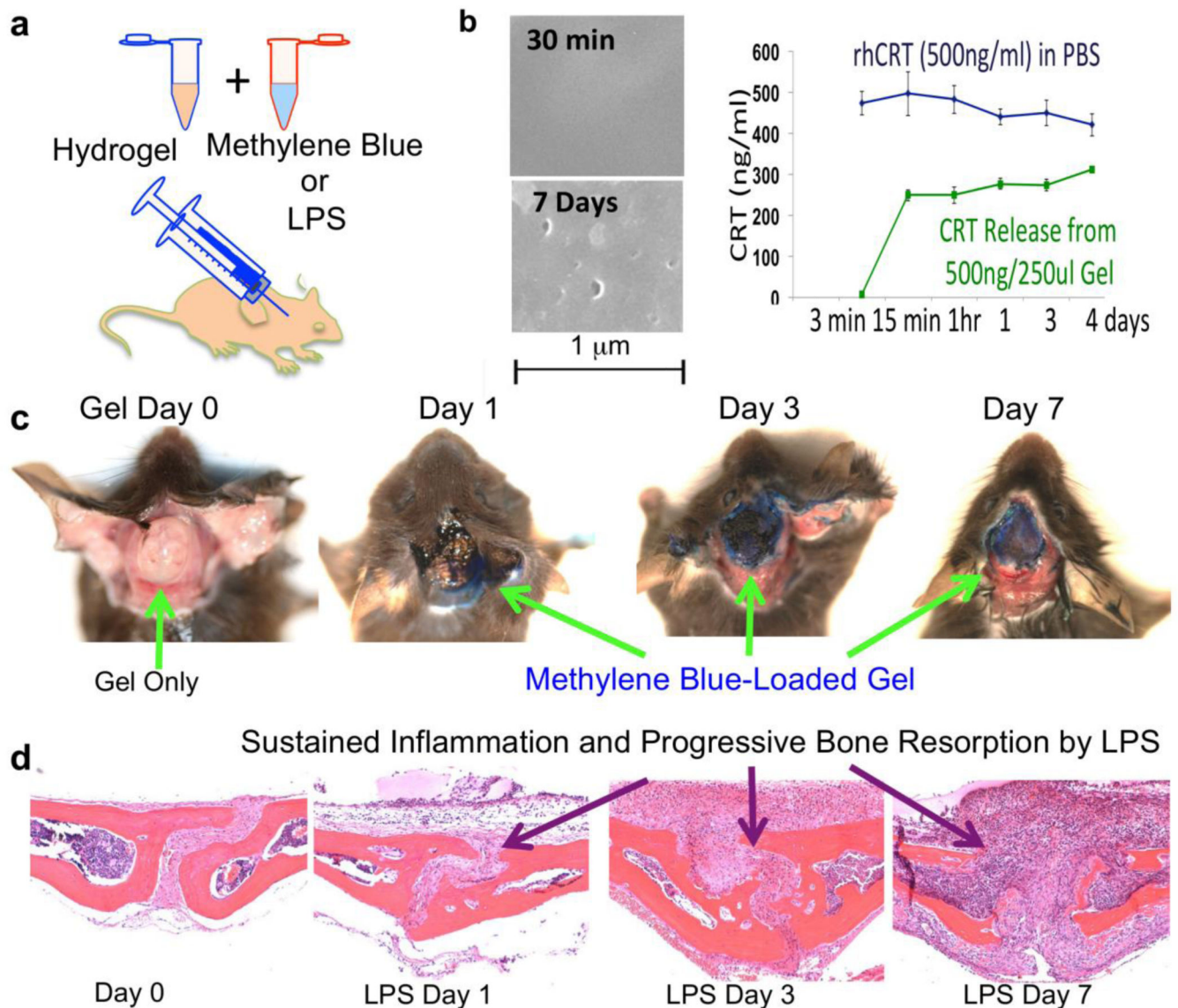
Kappa Delta Sorority for recognizing the importance of musculoskeletal research

American Academy of Orthopaedic Surgeons, Orthopaedic Research Society, and Orthopaedic Research & Education Foundation for guiding research and career development

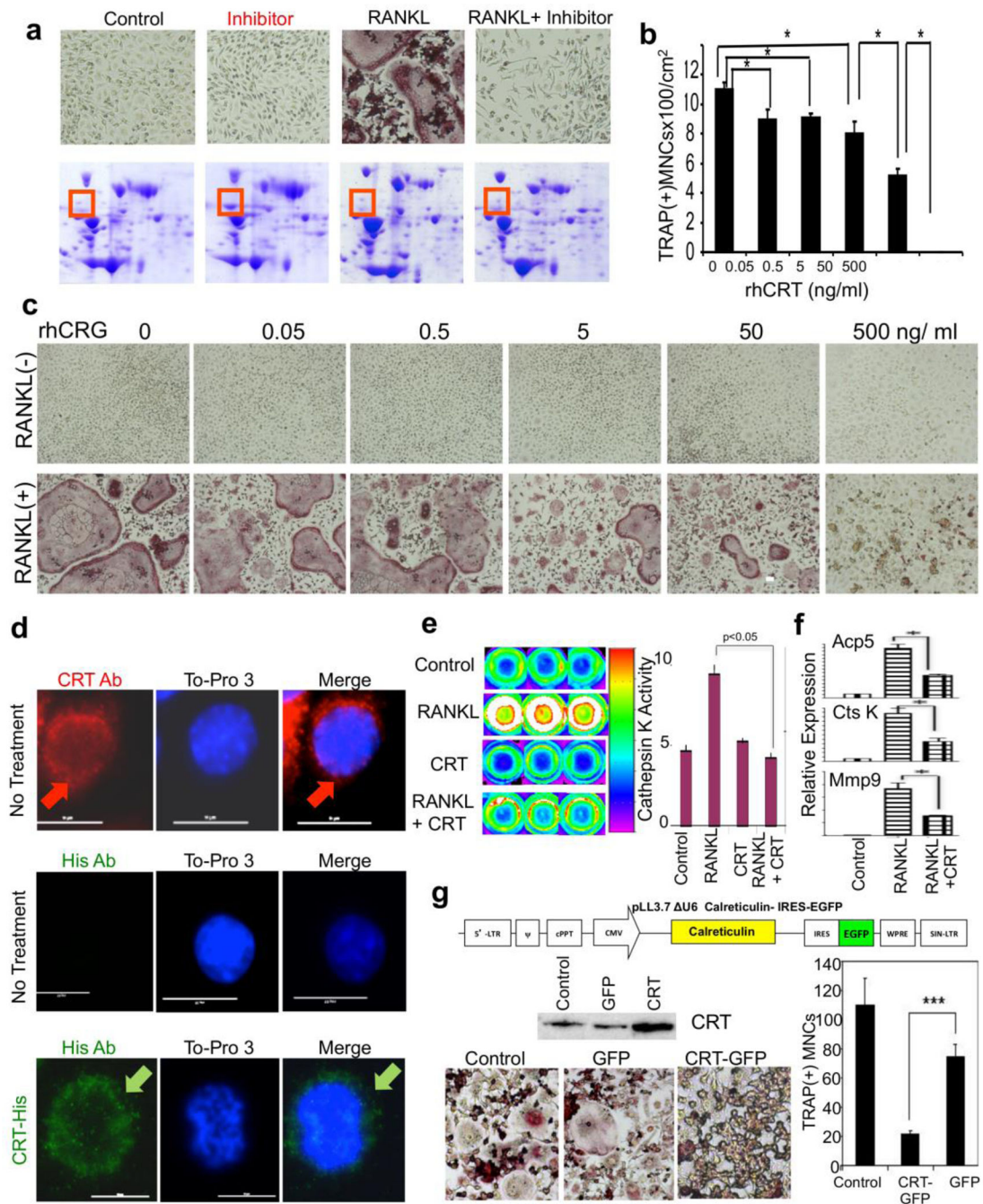
References

1. Teitelbaum SL. 2000; Bone Resorption by Osteoclasts. *Science*. 289: 1504–1508. [PubMed: 10968780]
2. Wei S, Kitaura H, Zhou P, et al. 2005; IL-1 mediates TNF-induced osteoclastogenesis. *The Journal of clinical investigation*. 115: 282–290. [PubMed: 15668736]
3. Lambert C, Oury C, Dejardin E, et al. 2007; Further insights in the mechanisms of interleukin-1beta stimulation of osteoprotegerin in osteoblast-like cells. *Journal of bone and mineral research : the official journal of the American Society for Bone and Mineral Research*. 22: 1350–1361.
4. Mizoguchi F, Murakami Y, Saito T, et al. 2013; miR-31 controls osteoclast formation and bone resorption by targeting RhoA. *Arthritis Res Ther*. 15: R102. [PubMed: 24004633]
5. Teitelbaum SL. 2011; The osteoclast and its unique cytoskeleton. *Annals of the New York Academy of Sciences*. 1240: 14–17. [PubMed: 22172034]
6. Silva-Fernandez L, Hyrich K. 2014; Rheumatoid arthritis: When TNF inhibitors fail in RA--weighing up the options. *Nature reviews Rheumatology*. 10: 262–264.
7. Isaacs JD. 2010; The changing face of rheumatoid arthritis: sustained remission for all? *Nature reviews Immunology*. 10: 605–611.
8. Redlich K, Smolen JS. 2012; Inflammatory bone loss: pathogenesis and therapeutic intervention. *Nature reviews Drug discovery*. 11: 234–250. [PubMed: 22378270]
9. Kong YY, Yoshida H, Sarosi I, et al. 1999; OPGL is a key regulator of osteoclastogenesis, lymphocyte development and lymph-node organogenesis. *Nature*. 397: 315–323. [PubMed: 9950424]
10. Schwarz EM, Ritchlin CT. 2007; Clinical development of anti-RANKL therapy. *Arthritis Res Ther*. 9 (Suppl 1) S7.
11. Bridgeman MB, Pathak R. 2011; Denosumab for the reduction of bone loss in postmenopausal osteoporosis: a review. *Clin Ther*. 33: 1547–1559. [PubMed: 22108301]
12. Brown-Glaberman U, Stopeck AT. 2012; Role of denosumab in the management of skeletal complications in patients with bone metastases from solid tumors. *Biologics*. 6: 89–99. [PubMed: 22532777]
13. Matsushita Y, Hayashida S, Morishita K, et al. 2016; Denosumab-associated osteonecrosis of the jaw affects osteoclast formation and differentiation: Pathological features of two cases. *Mol Clin Oncol*. 4: 191–194. [PubMed: 26893859]
14. Potts JT. 2005; Parathyroid hormone: past and present. *J Endocrinol*. 187: 311–325. [PubMed: 16423810]
15. Yang R, Hoang BH, Kubo T, et al. 2007; Over-expression of parathyroid hormone Type 1 receptor confers an aggressive phenotype in osteosarcoma. *International journal of cancer Journal international du cancer*. 121: 943–954. [PubMed: 17410535]
16. Zamanian M, Veerakumarasivam A, Abdullah S, Rosli R. 2013; Calreticulin and cancer. *Pathol Oncol Res*. 19: 149–154. [PubMed: 23392843]
17. Jia XY, He LH, Jing RL, Li RZ. 2009; Calreticulin: conserved protein and diverse functions in plants. *Physiol Plant*. 136: 127–138. [PubMed: 19453510]
18. Jia XY, Xu CY, Jing RL, et al. 2008; Molecular cloning and characterization of wheat calreticulin (CRT) gene involved in drought-stressed responses. *J Exp Bot*. 59: 739–751. [PubMed: 18349049]
19. Gold LI, Eggleton P, Sweetwyne MT, et al. 2010; Calreticulin: non-endoplasmic reticulum functions in physiology and disease. *FASEB J*. 24: 665–683. [PubMed: 19940256]
20. Mesaeli N, Nakamura K, Zvaritch E, et al. 1999; Calreticulin is essential for cardiac development. *J Cell Biol*. 144: 857–868. [PubMed: 10085286]
21. Obeid M, Tesniere A, Ghiringhelli F, et al. 2007; Calreticulin exposure dictates the immunogenicity of cancer cell death. *Nat Med*. 13: 54–61. [PubMed: 17187072]
22. Nanney LB, Woodrell CD, Greives MR, et al. 2008; Calreticulin enhances porcine wound repair by diverse biological effects. *Am J Pathol*. 173: 610–630. [PubMed: 18753412]

23. Patel N, Nizami S, Song L, et al. 2014. CA-074Me compound inhibits osteoclastogenesis via suppression of the NFATc1 and c-Fos signaling pathways. *Journal of orthopaedic research : official publication of the Orthopaedic Research Society*.
24. Seo SW, Lee D, Minematsu H, et al. 2010; Targeting extracellular signal-regulated kinase (ERK) signaling has therapeutic implications for inflammatory osteolysis. *Bone*. 46: 695–702. [PubMed: 19895919]
25. Asagiri M, Sato K, Usami T, et al. 2005; Autoamplification of NFATc1 expression determines its essential role in bone homeostasis. *The Journal of experimental medicine*. 202: 1261–1269. [PubMed: 16275763]
26. Hogan PG, Chen L, Nardone J, Rao A. 2003; Transcriptional regulation by calcium, calcineurin, and NFAT. *Genes & development*. 17: 2205–2232. [PubMed: 12975316]
27. Takayanagi H. 2007; The role of NFAT in osteoclast formation. *Annals of the New York Academy of Sciences*. 1116: 227–237. [PubMed: 18083930]
28. Kartsogiannis V, Ng KW. 2004; Cell lines and primary cell cultures in the study of bone cell biology. *Molecular and cellular endocrinology*. 228: 79–102. [PubMed: 15541574]
29. Aguda AH, Panwar P, Du X, et al. 2014; Structural basis of collagen fiber degradation by cathepsin K. *Proceedings of the National Academy of Sciences of the United States of America*. 111: 17474–17479. [PubMed: 25422423]
30. Ostwald TJ, MacLennan DH, Dorrington KJ. 1974; Effects of cation binding on the conformation of calsequestrin and the high affinity calcium-binding protein of sarcoplasmic reticulum. *J Biol Chem*. 249: 5867–5871. [PubMed: 4472093]
31. Basu S, Binder RJ, Ramalingam T, Srivastava PK. 2001; CD91 is a common receptor for heat shock proteins gp96, hsp90, hsp70, and calreticulin. *Immunity*. 14: 303–313. [PubMed: 11290339]
32. Dai E, Stewart M, Ritchie B, et al. 1997; Calreticulin, a potential vascular regulatory protein, reduces intimal hyperplasia after arterial injury. *Arterioscler Thromb Vasc Biol*. 17: 2359–2368. [PubMed: 9409202]
33. Arai A, Mizoguchi T, Harada S, et al. 2012; Fos plays an essential role in the upregulation of RANK expression in osteoclast precursors within the bone microenvironment. *J Cell Sci*. 125: 2910–2917. [PubMed: 22454522]
34. Mataraza JM, Li Z, Jeong HW, et al. 2007; Multiple proteins mediate IQGAP1-stimulated cell migration. *Cell Signal*. 19: 1857–1865. [PubMed: 17544257]
35. Meyer RD, Sacks DB, Rahimi N. 2008; IQGAP1-dependent signaling pathway regulates endothelial cell proliferation and angiogenesis. *PLoS One*. 3: e3848. [PubMed: 19050761]
36. Urao N, Razvi M, Oshikawa J, et al. 2010; IQGAP1 is involved in post-ischemic neovascularization by regulating angiogenesis and macrophage infiltration. *PLoS One*. 5: e13440. [PubMed: 20976168]
37. Ong CH, Bateman A. 2003; Progranulin (granulin-epithelin precursor, PC-cell derived growth factor, acrogranin) in proliferation and tumorigenesis. *Histol Histopathol*. 18: 1275–1288. [PubMed: 12973694]
38. Tang W, Lu Y, Tian QY, et al. 2011; The growth factor progranulin binds to TNF receptors and is therapeutic against inflammatory arthritis in mice. *Science*. 332: 478–484. [PubMed: 21393509]
39. Takayanagi H, et al. Induction and activation of the transcription factor NFATc1 (NFAT2) integrate RANKL signaling in terminal differentiation of osteoclasts. *Dev Cell*. 2002; 3 (6) 889–901. [PubMed: 12479813]
40. Kuroda Y, et al. Osteoblasts induce Ca²⁺ oscillation-independent NFATc1 activation during osteoclastogenesis. *Proc Natl Acad Sci U S A*. 2008; 105 (25) 8643–8. [PubMed: 18552177]
41. Kim H, et al. Tmem64 modulates calcium signaling during RANKL-mediated osteoclast differentiation. *Cell Metab*. 2013; 17 (2) 249–60. [PubMed: 23395171]

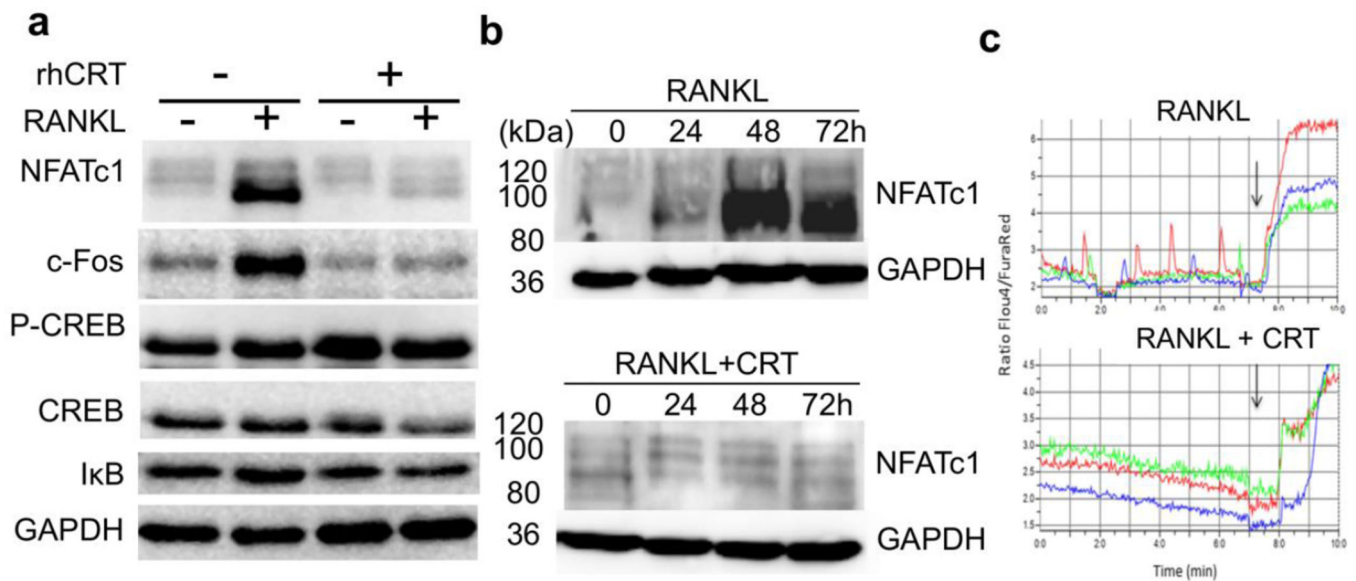
**FIGURE 1.**

Sustained inflammation model and drug delivery by hydrogel. **a.** Hydrogel is mixed with methylene blue, to demonstrated localized release, or LPS, to induce sustained inflammation and injected percutaneously over the calvaria. **b.** Scanning electron microscopy of hydrogel after 30mins and 7 days to demonstrate physical breakdown of gel corresponding to the release kinetics of CRT from the gel (right). **c.** Methylene blue loaded hydrogel displayed persistent localized release over 7 days. **d.** LPS loaded hydrogel instigates sustained inflammation leading to progressive bone resorption on the mouse calvaria.

**FIGURE 2.**

Identification of Calreticulin and inhibition of inflammatory osteolysis in vitro. **a.** Proteomic screening identified Calreticulin (CRT) as a potential inhibitor of osteoclastogenesis. Murine bone marrow derived macrophages (BMMs) treated with M-CSF alone (control), caspase-1 inhibitor Ac-YVAD-CMK (Inhibitor), RANKL, or RANKL plus Ac-YVAD-CMK (RANKL+Inhibitor) for 72 hours. The whole cell lysates were subjected to 2-D gel electrophoresis and stained with coomassie blue. The red boxes indicate the differentially expressed protein that was later identified as Calreticulin by mass-spec. **b-c.** Quantification

of panel c (*:p < 0.05), an in vitro osteoclastogenic model using RAW264.7 cells treated with and without RANKL which demonstrates higher and higher inhibitory effect on osteoclastogenesis as rhCRT dose is increased. **d.** Immunofluorescent staining of endogenous and exogenous CRT in murine BMMs. Top panel: endogenous CRT was stained red with an anti-CRT antibody, and nucleus was visualized with To-Pro3. Red arrows indicate peri-nuclear endoplasmic reticulum CRT staining. Middle panel: anti-His antibody showed negative staining of endogenous CRT in untreated BMMs; bottom panel: anti-His antibody revealed exogenous His-rhCRT internalized by BMMs. Green arrows indicate internalized His-tagged CRT. **e.** CRT inhibited Cathepsin K's activity in BM derived osteoclasts. Mouse bone marrow osteoclast precursors were treated with RANKL (RL) in the absence or presence CRT for 4 days in triplicate. Cathepsin K activity was imaged (left panel) and quantified (right panel). Red fluorescent indicates a higher activity. **f.** Expressions of osteoclast specific genes were quantified by qRT-PCR on BM osteoclasts after 3 days of RANKL (RL) or RANKL+CRT (RL+CRT). Acp5: TRAP, CtsK: cathepsin K, Mmp9: matrix metalloproteinase 9. **g.** Over-expression of CRT also inhibited osteoclastogenesis. TOP: Lentiviral construct used to overexpress CRT in primary mouse cells. MIDDLE: CRT expression in CRT-lentiviral transfected RAW264.7 cells was increased compared to untransfected control as well as empty vector transfected (GFP) transfected cell. BOTTOM LEFT: TRAP stained RAW264.7 cell derived osteoclasts that were either untransduced (control), transduced with empty lentivirus (GFP), or CRT-lentivirus after 4 days with RANKL; BOTTOM RIGHT: a quantification of left panel to show number of osteoclasts. ***:p < 0.001.

**FIGURE 3.**

Recombinant human calreticulin (rhCRT) inhibited key transcription factors and calcium oscillation during osteoclastogenesis. **a.** Raw264.7 cells were either untreated or treated with RANKL with or without 500ng/ml of rhCRT for 3 days, whole cell extracts were separated by SDS-PAGE and blotted for different antibodies against NFATc1, c-Fos, phospho-CREB, total CREB, IκB, and GAPDH, respectively. **b.** RAW264.7 cells were treated with RANKL alone (top) or with rhCRT (bottom) for 3 days, total cell lysates were made every 24 hours and subjected to SDS-PAGE and probed with NFATc1 and GAPDH antibodies. The numbers on the left indicate the molecular weight. **c.** Calreticulin inhibits cell Ca²⁺ oscillation. Mouse bone marrow derived macrophages were treated with M-CSF and RANKL without CRT (top) or with rhCRT (bottom) for 3 days. The cells were labeled with Fluo-4 AM and FuraRed and Ca²⁺ oscillation signal was presented as ratio of Fluo-4 AM to FuraRed fluorescent intensity. Each color line represented an individual cell in the same field. Arrows indicate when ionomycin was added.

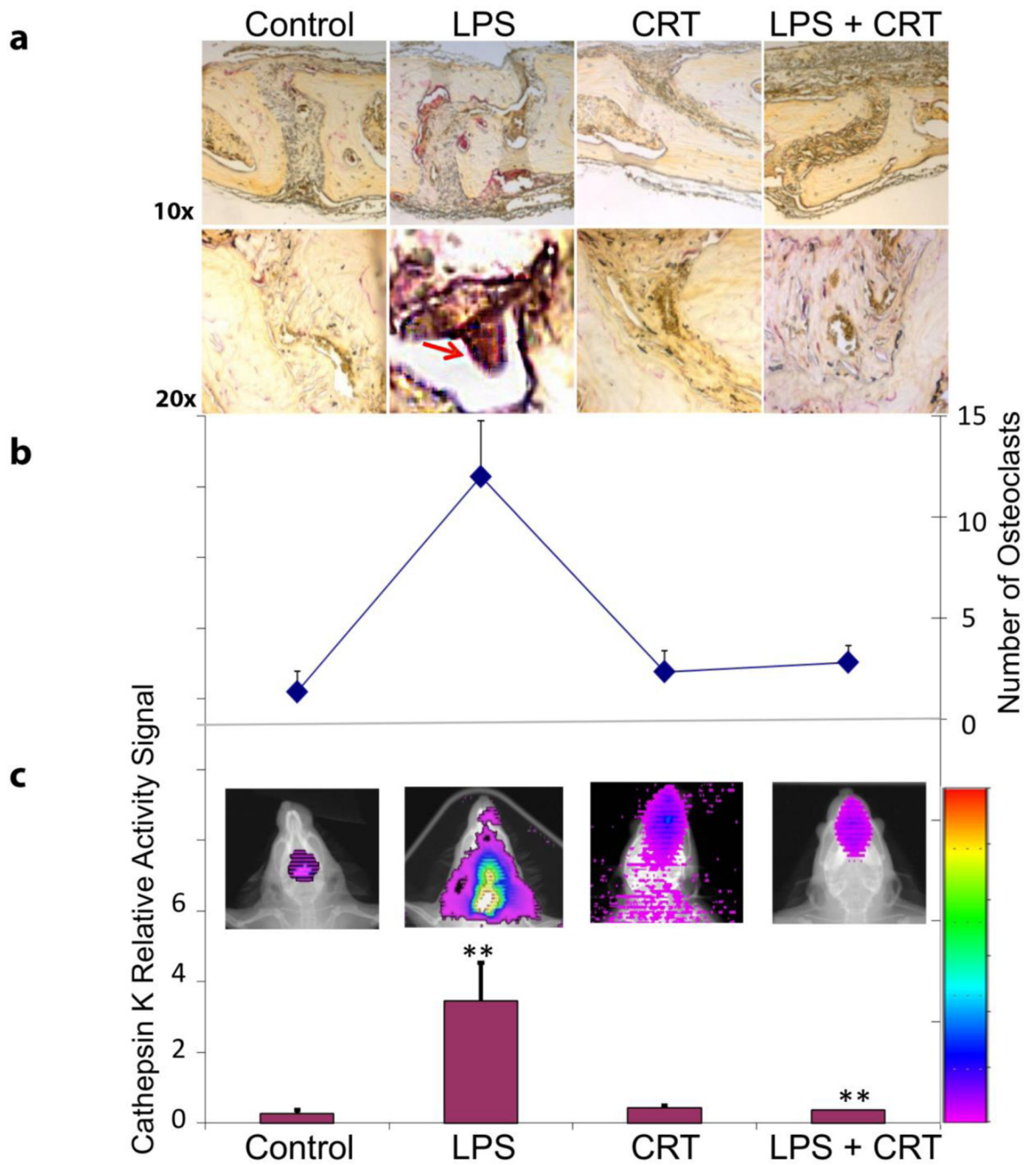


FIGURE 4. Functional osteoclast imaging detecting Cathepsin K activities and effect of exogenous CRT on LPS-induced osteoclastogenesis in vivo (N=6; $p < 0.05$; Day 3; Red Arrow: Osteoclastic bone resorption).

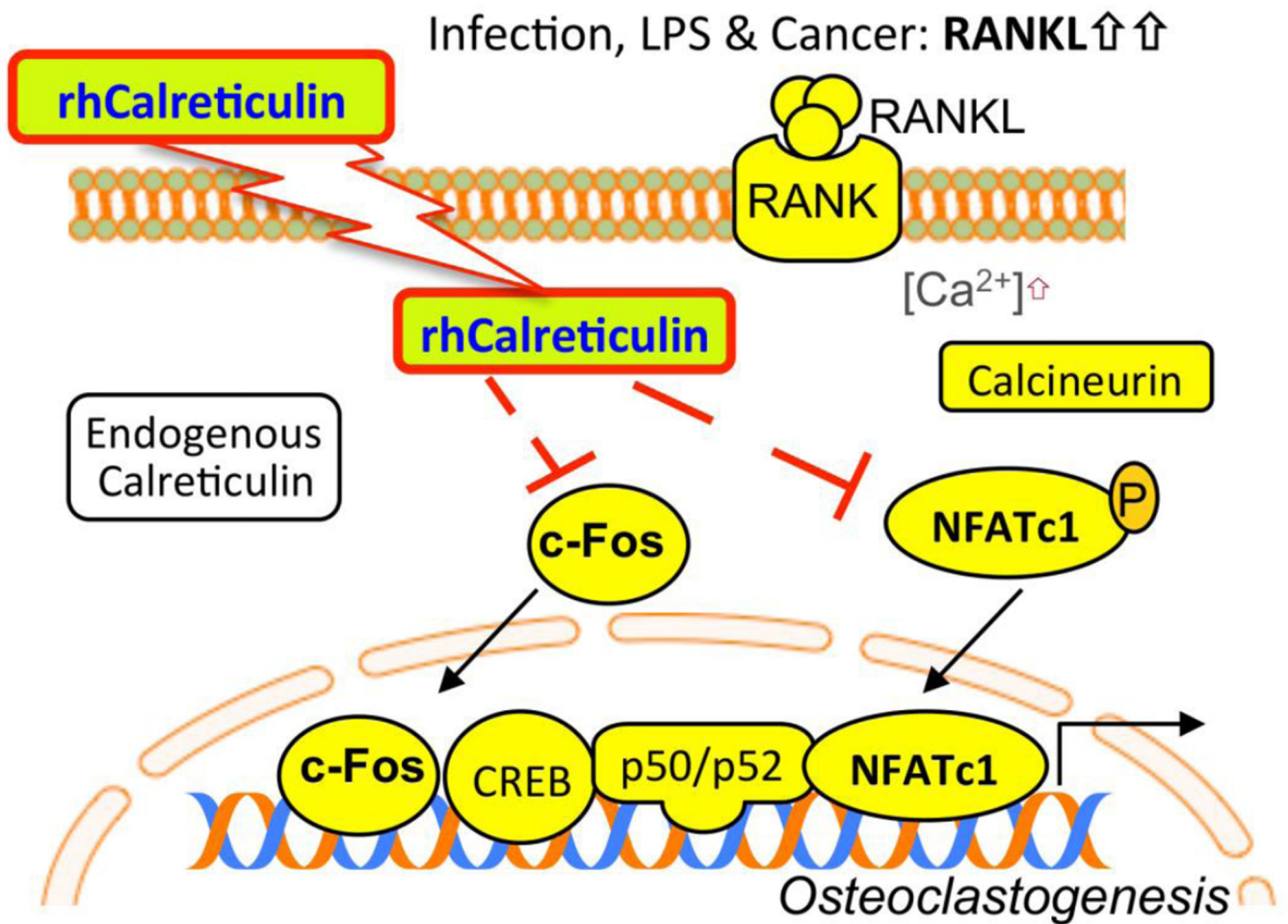


FIGURE 5.

Possible mechanistic summation of our results. Recombinant human Calreticulin is moved or is able to move through the cell membrane. Once inside a cell that is undergoing RANKL mediated Ca^{2+} oscillation, resulting in NFATc1 and c-Fos activity, the exogenous Calreticulin moves to inhibit NFATc1 and c-Fos. This results in the cessation of the NFATc1 auto-amplification which drives osteoclast differentiation and results in osteoclast specific gene expression.